Photovoltaic Hot-Spots Fault Detection Algorithm using Fuzzy Systems

Mahmoud Dhimish, *Member, IEEE,* & Ghadeer Badran*, Member, IEEE*

Abstract—**Faults in photovoltaic (PV) modules, which might result in energy loss and reliability problems are often difficult to avoid, and certainty need to be detected. One of the major reliability problems affecting PV modules is hot-spotting, where a cell or group of cells heats up significantly compared to adjacent solar cells, hence decreasing the optimum power generated. In this article, we propose a fault detection of PV hot-spots based on the analysis of 2580 PV modules affected by different types of hot-spots, where these PV modules are operated under various environmental conditions, distributed across the UK. The fault detection model comprises a fuzzy inference system (FIS) using Mamdani-type fuzzy controller including three input parameters, namely, percentage of power loss (PPL), short circuit current (I_{sc}), and open circuit voltage (V_{oc}). In order to test the effectiveness of the proposed algorithm, extensive simulation and experimental-based tests have been carried out; while the average obtained accuracy is equal to 96.7%.**

Index Terms—**Photovoltaic; Hot-Spots; Fault Detection; I-V curve; Fuzzy Logic; Power Loss.**

I. INTRODUCTION

HOT-SPOTTING phenomena is a reliability issue in Photovoltaic (PV) panels, where it is well-acknowledged when a dissenting solar cell heats up considerably and decreases the PV panel generated power [1]. PV hot-spotting arise when a single-cell, or group of cells operates at reverse-bias, and accordingly functioning at abnormal elevated temperature levels [2] and [3]. The hot-spots are also the key reason of enhanced PV degradation, and occasionally permanent damage of a complete PV panels [4]. There are a number of other reliability problems affecting PV panels such as discontinuation [5], maximum power point tracking (MPPT) faults [6] and [7], micro-cracks [8], and variations in the wind speed and humidity [9]. All of these factors affect the PV panels output power performance and its main electrical parameters such as temperature coefficient, hence diminution its annual energy production. Nevertheless, this article only addresses the impact of hot-spotting in PV panels, while other issues has not been addressed.

PV hot-spots can simply be observed using infrared (IR) camera inspection, which has become a common practice in current PV examination as presented in [10]. Still, the impact of hot-spots on the performance of PV systems have not considerably been addressed. This helps us to clarify why there is a lack of accepted methods which reflects to the hot-spotting as well as detailed standards referring to the rejection or acceptance benchmark in commercial frameworks.

The generally practice accepted of hot-spotting effects mitigation is by the adoption of bypass diodes which are connected within the PV modules, with the target to edge the extreme reverse voltage across the hot-spotted solar cells, this use of bypass diodes enhances the amount of short circuit current and the open circuit voltage of the affected PV panel [11] – [13], which is not ideal, since it necessitates extra cost and can be even detrimental in terms of power dissipation initiated by the added bypass diodes as discussed in [14].

Recently, a distributive MPPT technique suggested by Coppola *et al.* [15] and Olalla *et al.* [16], to mitigate hot-spots in PV modules, yielded an estimated decrease of 20 °C for medium and small hot-spotting regions. Additionally, Kim and Krein [17] show the "inadequateness" of the typical bypass diodes, by the addition of a series connected switch which are suitable to interpose the flow of the current during bypass activation process. However, this solution needs a moderately complex electronic-based design.

In 2018, two hot-spot mitigation methods are established by Dhimish *et al.* [18]. Based on MOSFETs associated to the PV panels in order to regulator the hot-spotted PV solar string. The suggested techniques verified reliable, but do not comprise any analysis for the overall impact of PV hot-spots on the output power performance.

The main contribution of this work, is to firstly study and analyse the impact of PV hot-spotting using the percentage of power loss (PPL) technique. The analysis not only deliberates local PV modules mounted at specific geographical locations, but also PV modules distributed across all UK regions; with a subtotal of 2580 examined PV modules. Hence, the analysis discussed in this article consider PV modules affected by completely different environmental conditions. Secondly, we propose the development of a suitable PV hot-spot fault detection algorithm using Mamdani fuzzy inference system (FIS). Finally, evaluate the proposed algorithm using various PV modules affected by diverse types of hot-spots.

The article is prearranged as follows: section II defines the methodology over the examined hot-spotted PV modules, while section III presents the proposed fuzzy logic based detection algorithm. Finally, section IV experimentally evaluates the proposed detection method.

Mahmoud Dhimish* and Ghadeer Badran are with the Department of Engineering and Technology, Photovoltaics Laboratory, University of Huddersfield, Huddersfield, HD1 3DH (Corresponding author (M. Dhimish) email: M.A.Dhimish@hud.ac.uk).

II. METHODOLOGY

A. Examined PV modules

The distributed PV installations studied dataset was supplied by Solar UK database [19], which has the PV panels' output current, voltage and generated power. The geographical-map presenting the scattering of the examined PV systems across the UK is shown in Fig. 1. The total inspected Polycrystalline Silicon (Poly-Si) PV panels within all examined PV systems are equal to 8340. The majority of the PV panels were fixed from 2005-2007, the PV panels were supplied by a mixture of commercial scale and homeowners PV installations, were their capacity varying from 1.1 and 50 kWp with a wide range of tilt and orientation angel.

The collection of the data was occupied on-site from multiple PV-based companies. The power-voltage (P-V) and current-voltage (I-V) curves were also available in the database. On the other hand, the instruments to trace P-V and I-V curves are subject to different measurement accuracy and tolerance rates. Therefore, the collected data were subjected to demanding validation and confirmation in order to eliminate as much inconsistent data as possible. The typical set of processes employed prior to data analysis stage are as follows:

- The PV modules P-V and I-V curves were captured during clear-sky, non-shading conditions as reported in the database.
- The PV installations have been inspected regularly by IR camera. Where the size of hot-spotted solar cells in each PV module can be counted and the location of the hot-spots is also identified.
- Take into account only PV systems installed in the UK as the available data contain a number of PV systems installed in a wide range of countries.
- Tilt angle of 30° to 60°, and orientation between -30° to +30°, only has been selected.
- Select PV systems with available individual PV module data; hence it is possible to compare between hot-spotted PV modules and adjacent non-hot-spotted/healthy PV modules.
- To eliminate inaccurate data, we have only taken into account PV systems which contain instruments and sensors within accuracy of 95% and above.

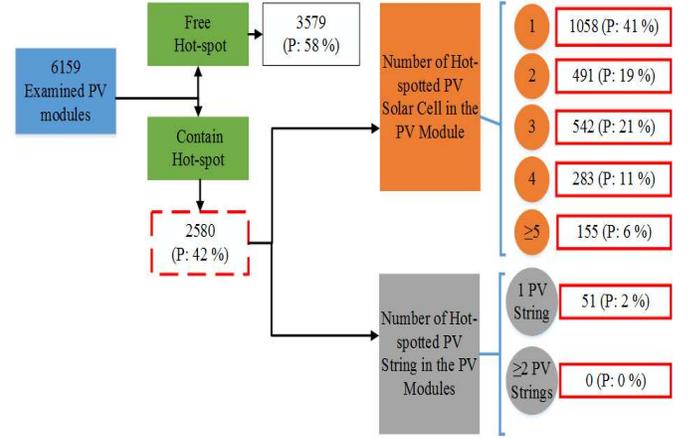Fig. 1. Geographical distribution of the examined PV systems

Fig. 2. Identified Hot-spots categories.

After selective requirements have been carried out, 6159 PV panels remain (out of 8340). The PV panels is shown in Fig. 2. The number of PV panels which did not comprise hot-spots were thus equal to 3579. While the number of hot-spotted PV modules are equal to 2580.

As shown in Fig. 2, the analysis of the hot-spots was analyzed based on the number of hot-spotted solar cells in the observed PV modules. Based upon the available datasets, the hot-spotted PV solar cells were categorized into two different sub-groups including PV modules affected by solar cells hot-spots, and PV modules affected by hot-spotted PV strings.

Fig. 3 demonstrates three different types of hot-spots. The hot-spots were inspected using a thermal imaging camera [20]. Fig. 3(a) presents a PV modules affected by one hot-spotted solar cell, where Figs. 3(b) and 3(c) show a PV module affected by two hot-spots and hot-spotted PV-string, respectively. In order to draw relevant outcomes, we have used the percentage of power loss (PPL) for each of the observed hot-spotting type, the technique is discussed in the next section.

B. Percentage of Power Loss (PPL) Technique

To examine the output power losses for hot-spotted PV modules, and since the PV modules have different output power capacity, the percentage of power loss (PPL) technique has been used.

Primarily, the measurement of the output power of the hot-spotted PV module is obtained ($P_{hot-spotted}$). This power is then to be divided by the average output power measured from adjacent free-hot-spotted/healthy PV modules. Adjacent PV modules average power is calculated using (1). Fig. 4 explains the valuation of the PPL technique.

$$P_{free} = \frac{\sum_{i=1}^{n} PV\ module\ Power}{n} \tag{1}$$

The calculations of the PPL including the measured and theoretical voltage and current are taken under STC conditions; where solar irradiance is equal to 1000 W/m^2, and ambient temperature of 25 °C.
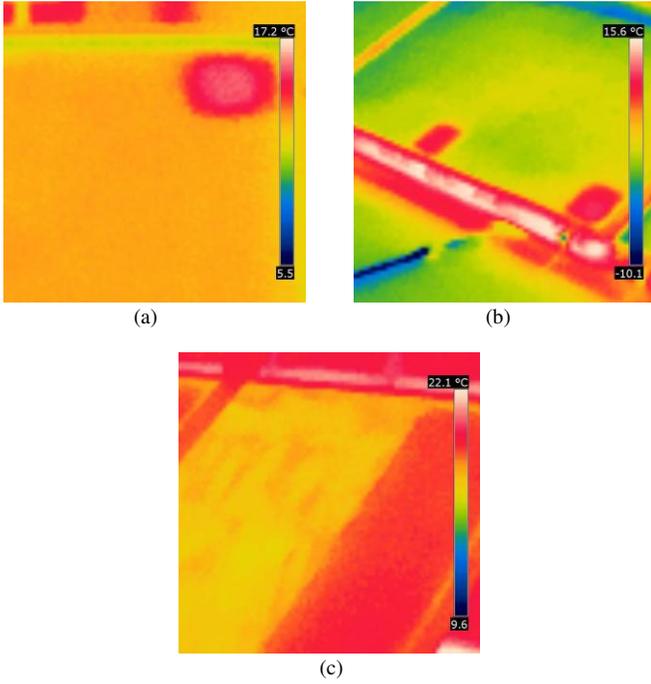
(a)

(b)

(c)

Fig. 3. Three different types of hot-spots affecting different PV modules. (a) One hot-spot, (b) Two hot-spots, (c) Hot-spotted PV string

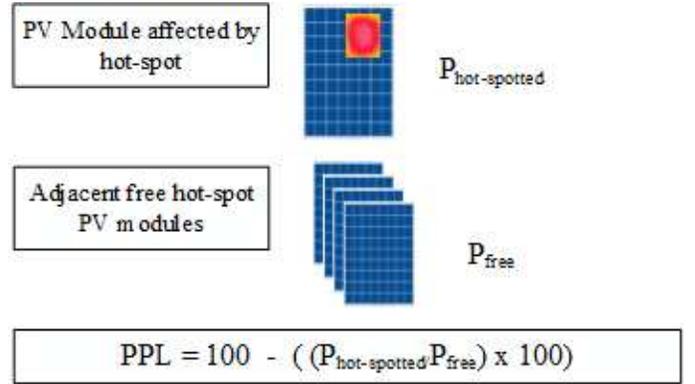$$PPL = 100 - ((P_{hot\text{-}spotted}/P_{free}) \times 100)$$

Fig. 4. Percentage of power loss (PPL) estimation for hot-spotted and non-hot-spotted/healthy PV modules

Interestingly, whilst increasing the hot-spots in PV modules, it is more likely to have greater drop in its output peak power, therefore, increase the percentage of the power loss (PPL) threshold. On the other hand, it is worth remembering that all listed PPL thresholds will be used to compromise the fuzzy logic inference system, hence, to detect possible hot-spotting category affecting a PV module.

The PPL is not the only parameter which is affected during hot-potting phenomena, but also the open circuit voltage (V_{oc}) and the short circuit current (I_{sc}). Example for the impact of two hot-spotted PV solar cells on the Isc and Voc are shown in Fig. 6(b) using the analysis of the I-V curve under standard test conditions. The examined PV module thermal image is presented in Fig. 6(a). As noticed, the percentage of reduction in the I_{sc} is equal to 2.05%, while the V_{oc} reduced by 1.1% compared to theoretical predictions. Therefore, the hot-spot cause a reduction in the I_{sc} and V_{oc}, accordingly these parameters are used in the developed PV detection system.

Table I shows a summary for the thresholds (minimum to maximum) reduction in the PPL, I_{sc} and V_{oc} for all inspected PV modules. As noticed, while increasing the hot-spots in the PV modules, the PPL, I_{sc} and V_{oc} reduces with higher degrees. But, as noticed there are overlapping between the thresholds (min – max) and hence it is unlikely to implement these thresholds into a proper hot-spotting fault detection algorithm using a mathematical or probabilistic modeling techniques. In order to overcome this issue, the implementation of a fuzzy logic inference system was adapted, eventually using the data presented in Table I with respect to three input parameters (PPL, I_{sc} and V_{oc}). In the next section there is a brief description of the implemented PV hot-spot detection system.

C. Analysis for PPL, I_{sc} and V_{oc} for the examined hot-spotted PV modules

Histogram profiles for the assessment of the determined data is shown in Fig. 5. The histogram comprises the measured PPL and the frequency of the PPL at definite thresholds. According to Fig. 5(a), it is evident that the PV modules affected by one hot-spotted solar cell have the minimum drop in the PPL; the average loss of the PPL is equal to 0.95%.

An increase in the number of hot-spotted solar cell resulting an increases in the PPL. For instance, Fig. 5(b) shows that the average PPL is equal to 2.0% for PV modules affected by two hot-spotted solar cells. These results are assessed over a sample size of 491 different PV modules. To sum up, the PPL thresholds (minimum to maximum) of all observed hot-spotting categories are summarized as follows:

- One hot-spot: 0.5% - 1.4%
- Two hot-spots: 1.1% - 2.9%
- Three hot-spots: 1.5 % - 3.8%
- Four hot-spots: 2.5% - 5.6%
- ≥5 hot-spots: 5.4% - 16.3%
- One hot-spotted PV string: 11.7% - 26.3%

Table I Thresholds (minimum to maximum) reduction in the PPL, I_{sc} and V_{oc} for all inspected PV modules

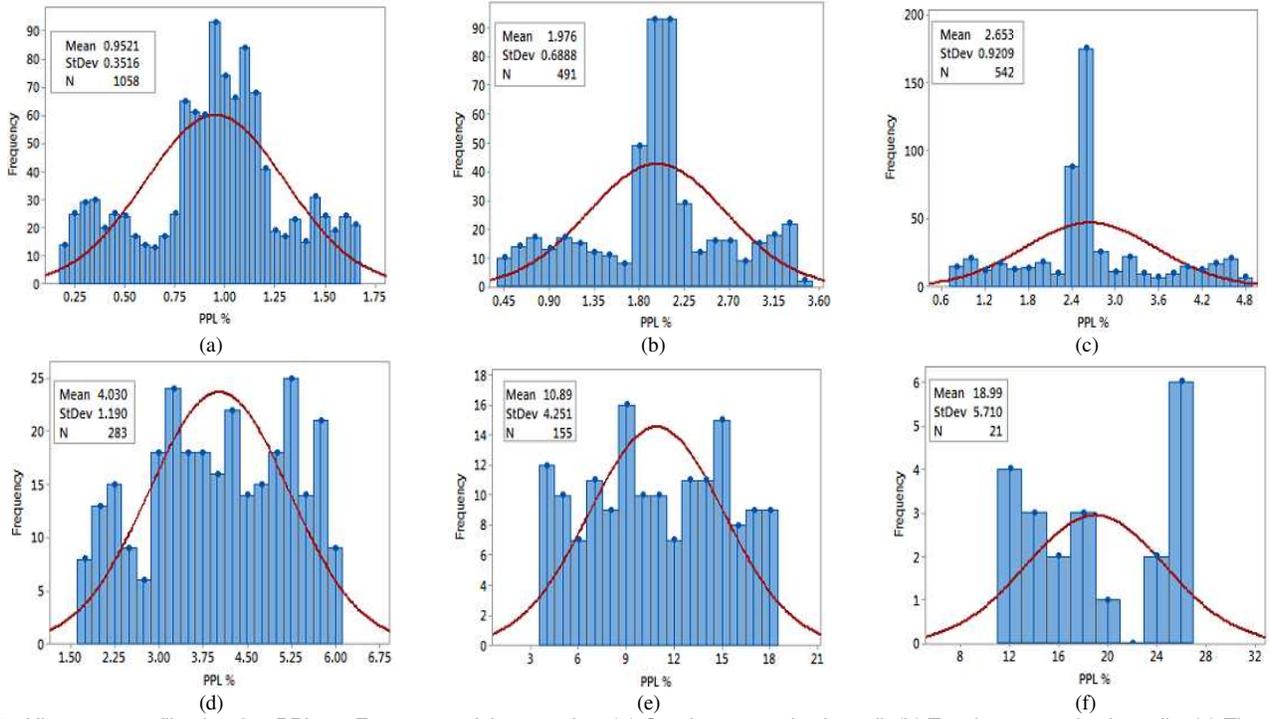| Hot-spotting Category	PPL		I_{sc}		V_{oc}	
	Minimum	Maximum	Minimum	Maximum	Minimum	Maximum
One hots-pot	0.5	1.4	0.7	1.5	0.3	0.8
Two hot-spots	1.1	2.9	0.95	2.3	0.65	1.8
Three hot-spots	1.5	3.8	1.3	2.7	1.4	2.2
Four hot-spots	2.5	5.6	1.33	2.9	1.7	2.7
≥5 Hot-spots	5.4	16.3	2.1	3.8	1.88	3.1
One Hot-spotted PV String	11.7	26.3	1.8	4.4	2.7	4.9

Fig. 5. Histogram profile showing PPL vs. Frequency of the samples. (a) One hot-spotted solar cell, (b) Two hot-spotted solar cells, (c) Three hot-spotted solar cells, (d) Four hot-spotted solar cells, (e) ≥5 hot-spotted solar cells, (f) Hot-spotted PV string in a PV module

III. PROPOSED PV HOT-SPOT DETECTION TECHNIQUE

A. FIS system modelling

A fuzzy inference system (FIS) is constructed using a fuzzy set theory, fuzzy reasoning, and the fuzzy rules. It is extensively useful for automatic control applications [21], time series estimation [22] and fault analysis [23]. In this article, we propose a suitable Mamdani FIS rather than strength of the Takgi-Sugeno-Kang (TSK) model, since Mamdani model can return output results which automatically express output results based on If-Then method; this method relies on determining whether an input parameter of the user belongs to the membership function using "If" and next convert the value into the fuzzy set using "Then". Adapting a direct interference between the measured inputs from the PV modules with the results of the detection system [24].

The fuzzy sets enlarge a present dataset using the concept of fuzzy logic. Each identified parameter has a gradation to which it belongs to the set (degree of membership). Generally, the degree of membership is expressed by a real number from 0 and 1. In this case, if a parameter corresponds to 1, therefore it does not belong to the set of 0. This can be express by (2).

$$A= \{(Q,\mu\_A (Q))\},0\leq\mu\_A (Q)\leq 1 \qquad (2)$$

where $\mu A(Q)$ is referred to as the membership function (MF) of the fuzzy set A, whereas the MF plays key role in the corresponding rudiments of the set Q for each value of the membership.

The knowledge-base of the Mamdani FIS consists of an adjusted rule and a database. The rule is built using the "linguistic rule" in the form of "If-Then". This rule has a fuzzy conditional criterion as follows:

$$\text{Rule1:} \quad \text{If v is A1 and x is B1 then z is C1} \qquad (3)$$

According to this rule, the output variable "z" is equal to C1 if both input variables v and x are only equal to A1 and B1, respectively. Hence, A1 and B1 are well-defined as the fuzzy values (fuzzy sets).
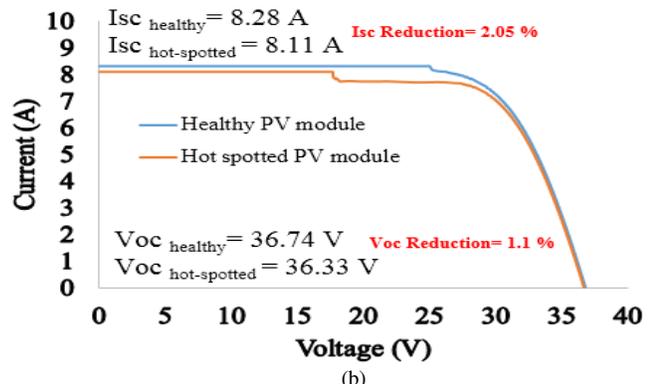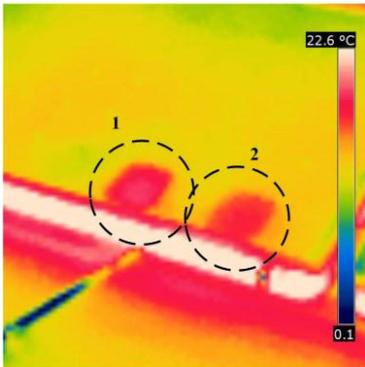

Fig. 6. (a) Thermal image of an inspected PV module, (b) Reduction in I_{sc} and V_{oc} for the PV module
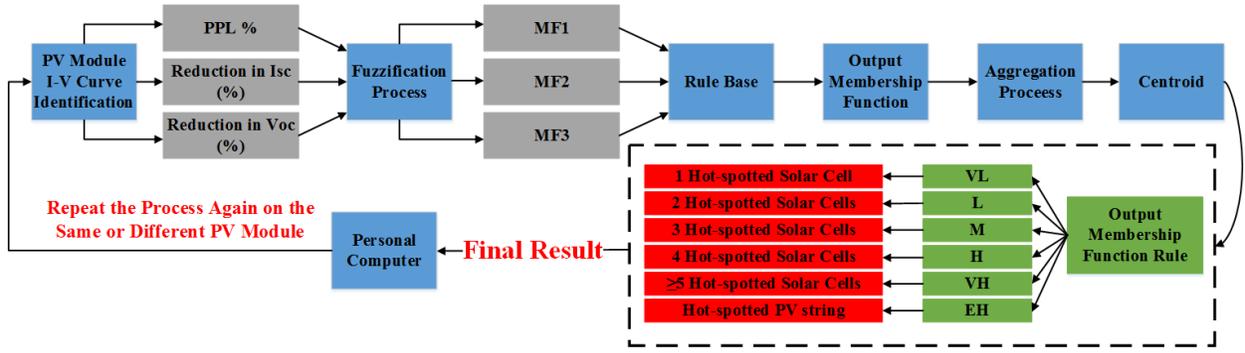
4

Fig. 7. Detained flowchart of the developed PV hot-spot detection system

An overview of the implemented fuzzy logic inference system for hot-spot PV detection is shown in Fig. 7, PPL, I_{sc} and V_{oc} are taken from the I-V curve of the inspected PV module. The Fuzzification process identifies the membership functions, and ultimately combines the measured PPL, I_{sc} and V_{oc}. The input membership functions are shown in Fig. 8(a-c); MF1 corresponds to PPL (interval: 0.5, 26.3), MF2 corresponds to I_{sc} (interval: 0.7, 4.4), and MF3 corresponds to V_{oc} (interval: 0.3, 4.9). All membership functions and their fuzzy sets are created using data available in Table I.

The FIS is used for the decision marking phase of the proposed fault detection algorithm. Under extreme scenarios, where the PPL, I_{sc} and V_{oc} has high variability and uncertainty, and the limits of the MFs level between the normal and fault operation mode of the PV system cannot be accurately well-defined, hence it would lower the accuracy of the overall FIS system. Therefore, the FIS rule based shown in Fig. 7 is determined by non-linear mapping of the three selected membership function features (MF1, MF2, and MF3), resulting an accurate representation for the output process.

Table II shows the extracted features of the fault conditions under different scenarios; where "VL, L, M, H, and VH" corresponds to "Very Low, Low, Medium, High, and Very High", respectively. Using "if-then" terminologies, the rule base defines the relation between the FIS inputs and outputs.

Next, the aggregation process shown in Fig. 7, comprises the output of the rules into a sole fuzzy set by means of the centroid method, which is a broadly used method in FIS [21] - [25], the obtained outputs of the aggregation are then defuzzified into actual output within 0 to 1 interval using (4).

$$Center\ of\ gravity = \frac{\int_a^b \mu_A(x)\,x\,dx}{\int_a^b \mu_A(x)} \tag{4}$$

where x indicates the sample element, and $\mu_A(x)$ is the membership function.

Further, by applying "If-Then", it is possible to generate the output MFs for the FIS as shown in Fig. 8(d). For example, if the PPL is from $0.5 - 1.4$ (MF1), and I_{sc} is from $0.7 - 1.5$ (MF2), and V_{oc} is from $0.3 - 0.8$ (MB3), then one hot-spotted solar cell is detected, labelled as VL (Very Low) in Fig. 8(d). Subsequently, the output membership functions correspond to the following features/hot-spotting category:

- Very Low (VL): one hot-spot
- Low (L): two hot-spots
- Medium (M): three hot-spots
- High (H): four hot-spots
- Very High (VH): ≥5 hot-spots
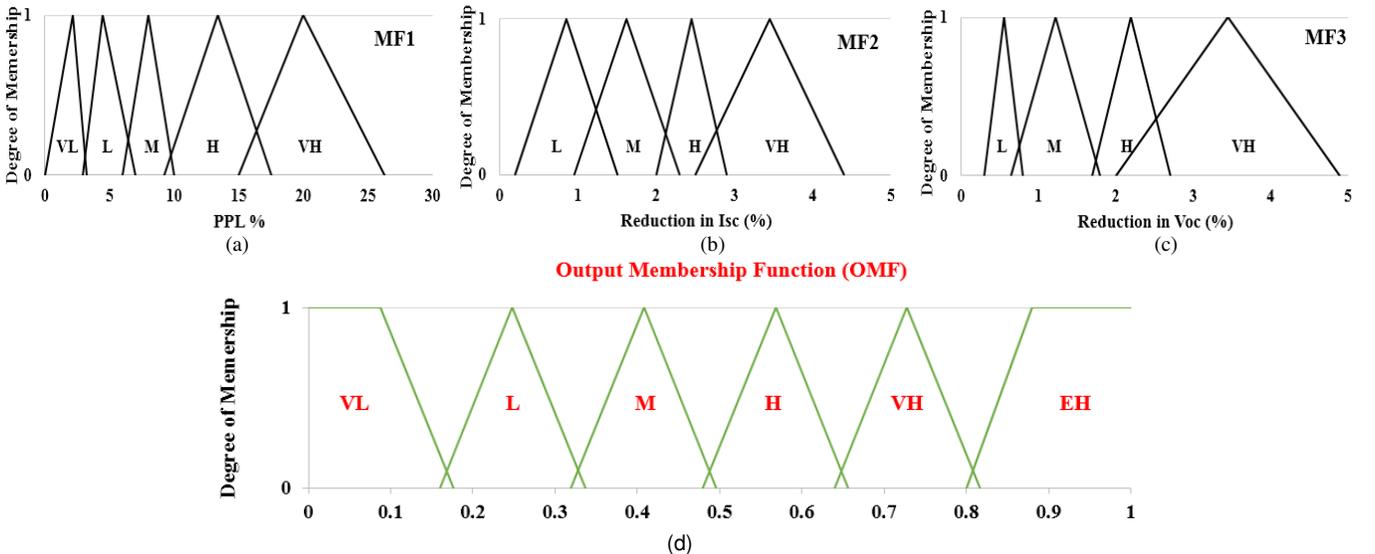- Extremely High (EH): hot-spotted PV string

Output Membership Function (OMF)

Fig. 8. (a) MF1 corresponds to PPL, (b) MF2 corresponds to I_{sc}, (c) MF3 corresponds to V_{oc}, (d) Output membership functions

5

Table II FIS rule base

Event	Features		
	MF1	MF2	MF2
One hot-spot	VL	L	L
Two hot-spots	L	M	L
Three hot-spots	M	M	M
Four hot-spots	M	H	H
≥5 hot-spots	H	VH	H
Hot-spotted PV string	VH	VH	VL

B. FIS system validation

In order to evaluate the performance of the developed FIS system, case studies were carried output using MATLAB/Simulink software packages. A PV modules affected by various types of hot-spots were modelled and simulated; where the output results have been passed into the FIS to determine the type of the hot-spot. 6000 cases have been simulated under different temperature levels. The hot-spots temperature is varying from 35 °C to 105 °C, while the solar irradiance is varied between 100 to 1000 W/m²; 1000 simulation were carried out for each of the 6-types of hot-spots identified in this article. Resulting numerous fluctuations in the output PPL, I_{sc}, and V_{oc}. The output identification and the average accuracy of the FIS system is reported in Table III. The average detection accuracy of the FIS system is equal to 96.7%; while the optimum fault identification accuracy of 98.3% is achieved by predicting the first hot-spot category "1 hot-spot". Whereas the minimum detection accuracy of 94.7% is determined for the fifth scenario "≥5 hot spots".

By contrast with the above results, the FIS False Positive (FP) and False Negative (FN) are determined with minimal effect on the FIS performance; of course, there are a number of case where the FP or FN existed. However, the maximum fault detection percentage of the FP/FN is equal to 1.5% found while simulating the third case scenario "3 hot-spots". This precision of the FIS model is due to the optimum selection of the FIS base rules, as well as the input membership functions including the PLL, I_{sc}, and V_{oc}.

Table III Hot-spot fault identification results of 6000 simulated cases

| Hot-spot Category	Fault Identification %						Average Detection Accuracy %
	1 HS	2 HS	3 HS	4 HS	≥5 HS	HS String	
1 hot-spot	**98.3**	1.6	0.1	0	0	0	-
2 hot-spots	2.2	**96.6**	1.2	0	0	0	-
3 hot-spots	0.5	1.1	**96.9**	1.5	0	0	-
4 hot-spots	0.6	0.3	1.8	**96.2**	1.1	0	-
≥5 hot-spots	0	0	0.2	0.7	**94.7**	4.4	-
Hot-spotted PV string	0	0	0.2	1.1	1.4	**97.3**	-
	-	-	-	-	-	-	**96.7%**

IV. EXPERIMENTAL EVALUATION

A. Examined PV installation

In order to test the accuracy of the proposed PV hot-spot detection FIS system, multiple PV modules affected by hot-spots were firstly inspected. The PV installations is shown in Fig. 9(a), where the PV modules main electrical parameters including PV peak power, I_{sc} and V_{oc} at STC are also listed. The modules are connected to MPPT units, these MPPT units accurately measures the main parameters form the inspected PV modules where the accuracy is above 99%. Next, the I-V curve is estimated using the data enabled from the Ethernet cable connected to a personnel computer (PC). The internal configuration of a MPPT units are show in Fig. 9(b). Next, the proposed detection system will eventually evaluate the inspected PV module using the fuzzy logic controller, as a result indicate whether the PV module is affected by hot-spotting and also predicting the PV hot-spotting type.

B. Case study 1: only hot-spotted PV modules

In this case study, three PV modules affected only by hot-spotted solar cells were examined under STC, hence to justify the accuracy of the employed fuzzy inference system. As discussed earlier, the I-V curve were captured using the MPPT unit through the PC user interface, and then process the results using the detection system. The output features of the I-V curves are processed into the FIS system; practically speaking using MATLAB/Simulink software. Hence, the output membership function of the FIS model is obtained.

The I-V curve of the first inspected PV module is shown in
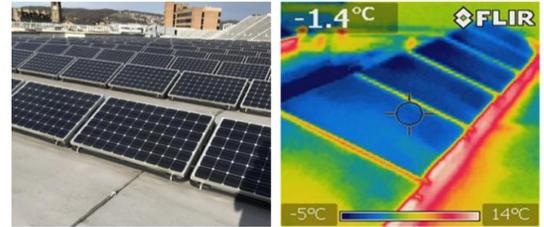
PV Modules Main Electrical Parameters:
Peak Power: 220.2 W
Voltage at maximum power point (V_{MPP}): 28.7 V
Current at maximum power point(I_{MPP}): 7.67 A
Open circuit voltage(V_{OC}): 36.7 V
Short circuit current(I_{SC}): 8.18 A

(a)

Adjustable Microcontroller — Input/output Pins

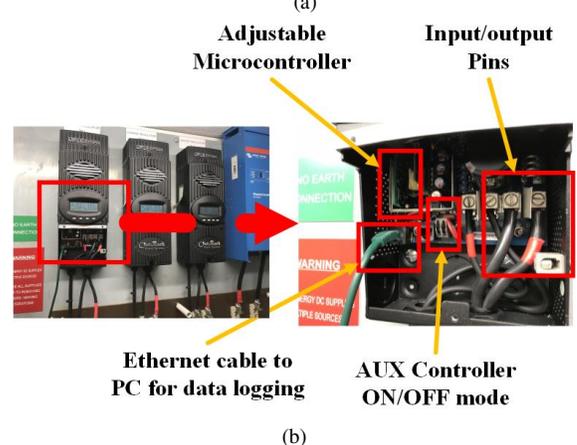Ethernet cable to PC for data logging — AUX Controller ON/OFF mode

(b)

Fig. 9. (a) Examined PV system real and thermal image, (b) Internal configuration of the MPPT unit

6

Fig. 10(a). The PPL, reduction in I_{sc} and V_{oc} are equal to 0.82%, 1.1% and 0.56%, respectively. Processing these parameters into the FIS resulting a VL (Very low: corresponds to one hot spotted solar cell in the PV module). In order to examine the result feature, we have captured the thermal image of the PV panel; shown in Fig. 10(d) first image. The thermal image clarifies that there is only one hot-spotted solar cell in the inspected PV module.
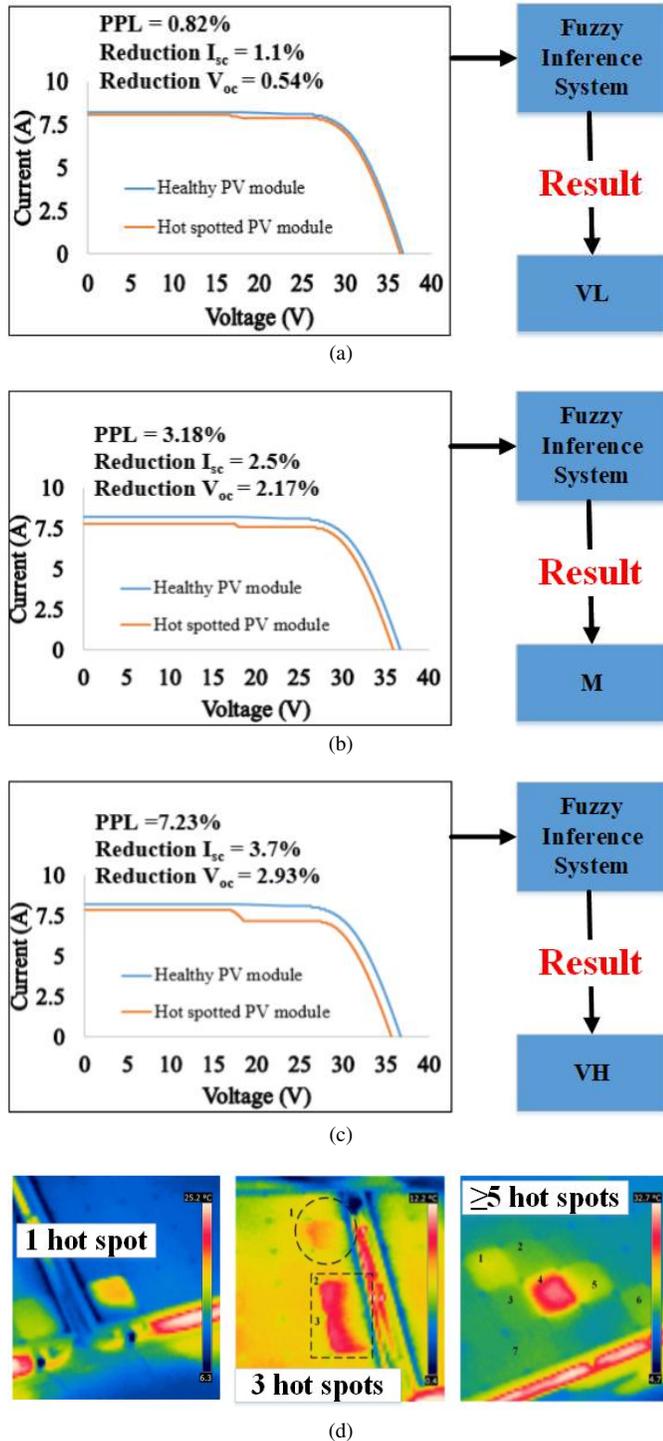

(a)

(b)

(c)

(d)

Fig. 10. I-V curve and FIS output for all inspected PV panels. (a) First PV panel, (b) Second PV panel, (c) Third PV module, (a) Thermal images for all inspected PV panels

Similarly, a second PV module was inspected and its output I-V curve is shown in Fig. 10(b). The FIS result indicates that there are three hot-spotted solar cells in the PV module (output membership function is M "Medium"). The second image in Fig. 10(d) demonstrates that there is three hot-spots in the inspected PV module.

The last example presenting ≥5 hot-spotted solar cells in a PV module is shown in last image in Fig. 10(d). The output of the FIS predicted this outcome using the result of the output membership function (VH "Very high") shown in Fig. 10(c).

C. Case study 2: hot-spotted PV modules and partial shading scenarios

This case study does not only consider hot-spotted PV module, but also a PV module that is affected by permanent shade. Generally, the source of the partial shade might be a cloud, tree, or building. In our case, the shade is caused by a ground pipe as shown in Fig. 11(a). In addition to the partial shade this pipe could cause, there are two hot-spots detected in the PV module using the thermal imaging.

According to Figs. 1 and 2, all inspected and filtered PV modules are captured under STC, and not partial shading scenarios were taken into account. Therefore, the predictions of the developed fuzzy inference system would not be expected to accurately identifying permanent partial shading conditions.

According to Fig. 11(b), the output membership function resulting a VH, corresponds to ≥5 hot-spotted solar cells in the PV module. Whereas the actual PV module is only affected by two hot-spots. There is a wrong identification in the type of the hot-spotting affecting the PV module due to the existence of a shade where this shade is not impacting adjacent (healthy) PV modules.
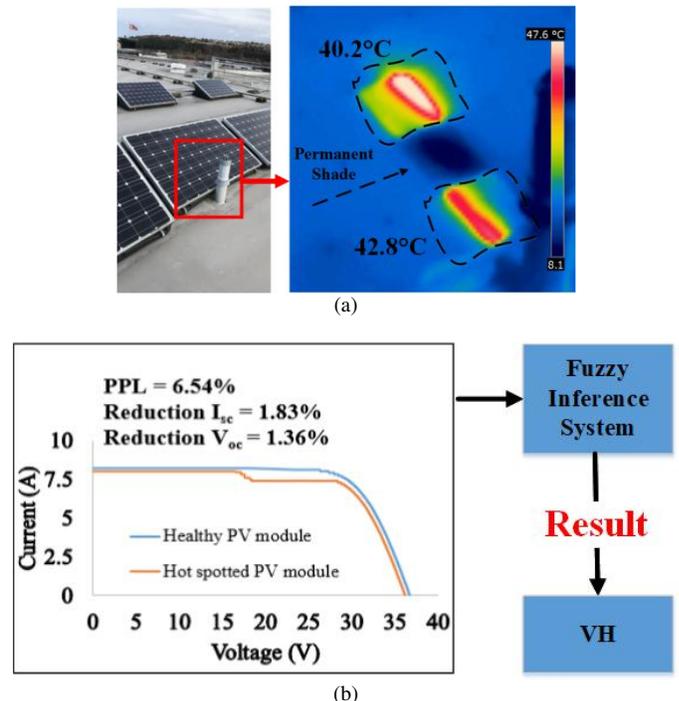

(a)

(b)

Fig. 11. (a) Examined PV module, real and thermal image, (b) I-V curve under STC

7

As a generic remark, the developed FIS method cannot identify hot-spotted PV module during partial shading conditions, but certainly PV module affected by only hot-spots will be accurately identified. Furthermore, if the inspected PV module is partially shaded and the adjacent/healthy PV modules are also partially shaded, in that case, the fault detection algorithm would work as expected, since the I-V curve for both the inspected (hot-spotted) and adjacent (healthy) PV modules will be have identical percentage of the loss in all required input parameters for the FIS model.

V. CONCLUSION

The problem in hot-spot fault detection of PV modules is addressed in this work. Under numerous types of conditions, e.g., various hot-spots types, different temperature levels, and different solar irradiance spectrum, the detection of hot-spotting is difficult to obtain, while this is not the case in the developed approach. We propose a fault detection of PV hot-spots based on the analysis of 2580 PV modules affected by different types of hot-spots, where these PV modules are operated under various environmental conditions, distributed across the UK. The fault detection model comprises a fuzzy inference system (FIS) using Mamdani-type fuzzy controller. There inputs of the FIS are determined including the percentage of power loss (PPL), open circuit voltage (V_{oc}), and short circuit current (I_{sc}). Extensive simulation has been carried out; while the average accuracy of the FIS is equal to 96.7%. In addition, multiple experiments have been conducted to assess the accuracy of the FIS system, where it was found that the develop method can precisely detect six-different types of hot-spotting affecting PV modules, whereas the main drawback of the developed algorithm that it is not capable of identifying hot-spots during high partial shading conditions.

REFERENCES

[1] M. Dhimish, V. Holmes, P. Mather, and M. Sibley, " Novel hot spot mitigation technique to enhance photovoltaic solar panels output power performance," in *Solar Energy Materials and Solar Cells,* vol. 179, pp. 72-79, June 2018, doi: 10.1016/j.solmat.2018.02.019.

[2] P. Mazumdar, P. N. Enjeti and R. S. Balog, "Analysis and Design of Smart PV Modules," in *IEEE Journal of Emerging and Selected Topics in Power Electronics*, vol. 2, no. 3, pp. 451-459, Sept. 2014, doi: 10.1109/JESTPE.2013.2294640.

[3] B. B. Pannebakker, A. C. De Waal, W. Van Sark, "Photovoltaics in the shade: one bypass diode per solar cell revisited," in Progress in Photovoltaics: Research and Applications, vol. 25, no. 10, pp. 836-849, 2017, doi: 10.1002/pip.2898.

[4] M. Simon, and E. L. Meyer, "Detection and analysis of hot-spot formation in solar cells," in *Solar Energy Materials and Solar Cells*, vol. 94, no. 2, pp. 106-113, 2010, doi: 10.1016/j.solmat.2009.09.016.

[5] V. V. S Pradeep Kumar and B. G. Fernandes, "A Fault-Tolerant Single-Phase Grid-Connected Inverter Topology With Enhanced Reliability for Solar PV Applications," in *IEEE Journal of Emerging and Selected Topics in Power Electronics*, vol. 5, no. 3, pp. 1254-1262, Sept. 2017, doi: 10.1109/JESTPE.2017.2687126.

[6] M. Rakhshan, N. Vafamand, M. Khooban and F. Blaabjerg, "Maximum Power Point Tracking Control of Photovoltaic Systems: A Polynomial Fuzzy Model-Based Approach," in *IEEE Journal of Emerging and Selected Topics in Power Electronics*, vol. 6, no. 1, pp. 292-299, March 2018, doi: 10.1109/JESTPE.2017.2708815.

[7] M. Dhimish, "70% decrease of hot-spotted photovoltaic modules output power loss using novel MPPT algorithm," in IEEE Transactions on Circuits and Systems II: Express Briefs, doi: 10.1109/TCSII.2019.2893533.

[8] M. Dhimish, V. Holmes, B. Mehrdadi, and M. Dales, "The impact of cracks on photovoltaic power performance," in *Journal of Science: Advanced Materials and Devices*, vol. 2, no. 2, pp. 199-209, 2017, doi: 10.1016/j.jsamd.2017.05.005.

[9] V. Stoichkov, D. Kumar, P. Tyagi and J. Kettle, "Multistress Testing of OPV Modules for Accurate Predictive Aging and Reliability Predictions," in *IEEE Journal of Photovoltaics*, vol. 8, no. 4, pp. 1058-1065, July 2018, doi: 10.1109/JPHOTOV.2018.2838438.

[10] Y. Hu, W. Cao, J. Ma, S. J. Finney and D. Li, "Identifying PV Module Mismatch Faults by a Thermography-Based Temperature Distribution Analysis," in *IEEE Transactions on Device and Materials Reliability*, vol. 14, no. 4, pp. 951-960, Dec. 2014, doi: 10.1109/TDMR.2014.2348195.

[11] G. Acciari, D. Graci and A. La Scala, "Higher PV Module Efficiency by a Novel CBS Bypass," in *IEEE Transactions on Power Electronics*, vol. 26, no. 5, pp. 1333-1336, May 2011, doi: 10.1109/TPEL.2010.2095469.

[12] K. A. Kim, G. Seo, B. Cho and P. T. Krein, "Photovoltaic Hot-Spot Detection for Solar Panel Substrings Using AC Parameter Characterization," in *IEEE Transactions on Power Electronics*, vol. 31, no. 2, pp. 1121-1130, Feb. 2016, doi: 10.1109/TPEL.2015.2417548.

[13] M. Dhimish, V. Holmes, B. Mehrdadi, M. Dales, and P. Mather, "PV output power enhancement using two mitigation techniques for hot spots and partially shaded solar cells," in *Electric Power Systems Research*, vol. 158, pp. 15-25, 2018, doi: 10.1016/j.epsr.2018.01.002.

[14] P. Manganiello, M. Balato and M. Vitelli, "A Survey on Mismatching and Aging of PV Modules: The Closed Loop," in *IEEE Transactions on Industrial Electronics*, vol. 62, no. 11, pp. 7276-7286, Nov. 2015, doi: 10.1109/TIE.2015.2418731.

[15] M. Coppola, S. Daliento, P. Guerriero, D. Lauria and E. Napoli, "On the design and the control of a coupled-inductors boost dc-ac converter for an individual PV panel," *International Symposium on Power Electronics Power Electronics, Electrical Drives, Automation and Motion*, Sorrento, 2012, pp. 1154-1159, doi: 10.1109/SPEEDAM.2012.6264548.

[16] C. Olalla, Md. Hasan, C. Deline, and D. Maksimovic, "Mitigation of Hot-Spots in Photovoltaic Systems Using Distributed Power Electronics," in *Energies*, vol. 11, no. 4, pp. 726, 2018, doi: 10.3390/en11040726.

[17] K. A. Kim and P. T. Krein, "Reexamination of Photovoltaic Hot Spotting to Show Inadequacy of the Bypass Diode," in *IEEE Journal of Photovoltaics*, vol. 5, no. 5, pp. 1435-1441, Sept. 2015, doi: 10.1109/JPHOTOV.2015.2444091.

[18] M. Dhimish, V. Holmes, B. Mehrdadi, M. Dales, and P. Mather, "Output-Power Enhancement for Hot Spotted Polycrystalline Photovoltaic Solar Cells," in *IEEE Transactions on Device and Materials Reliability*, vol. 18, no. 1, pp. 37-45, March 2018, doi: 10.1109/TDMR.2017.2780224.

[19] Solar Energy from SolarUK Ltd, 2019. Retrieved from: http://www.solaruk.com/.

[20] W. S. M. Brooks, D. A. Lamb and S. J. C. Irvine, "IR Reflectance Imaging for Crystalline Si Solar Cell Crack Detection," in *IEEE Journal of Photovoltaics*, vol. 5, no. 5, pp. 1271-1275, Sept. 2015, doi: 10.1109/JPHOTOV.2015.2438636.

[21] S. S. Khorramabadi and A. Bakhshai, "Intelligent Control of Grid-Connected Microgrids: An Adaptive Critic-Based Approach," in *IEEE Journal of Emerging and Selected Topics in Power Electronics*, vol. 3, no. 2, pp. 493-504, June 2015, doi: 10.1109/JESTPE.2014.2331188.

[22] S. Yin, Y. Jiang, Y. Tian and O. Kaynak, "A Data-Driven Fuzzy Information Granulation Approach for Freight Volume Forecasting," in *IEEE Transactions on Industrial Electronics*, vol. 64, no. 2, pp. 1447-1456, Feb. 2017, doi: 10.1109/TIE.2016.2613974.

[23] S. Roy, M. K. Alam, F. Khan, J. Johnson and J. Flicker, "An Irradiance-Independent, Robust Ground-Fault Detection Scheme for PV Arrays Based on Spread Spectrum Time-Domain Reflectometry (SSTDR)," in *IEEE Transactions on Power Electronics*, vol. 33, no. 8, pp. 7046-7057, Aug. 2018, doi: 10.1109/TPEL.2017.2755592.

[24] M. Dhimish, V. Holmes, B. Mehrdadi and M. Dales, "Comparing Mamdani Sugeno fuzzy logic and RBF ANN network for PV fault detection," in *Renewable Energy*, vol. 117, pp. 257-274, March 2018, doi: 10.1016/j.renene.2017.10.066.

[25] Y. K. Kang, H. Kim, G. Heo and S. Song, "Diagnosis of feedwater heater performance degradation using fuzzy inference system," in *Expert Systems with Applications*, vol. 69, pp. 239-246, March 2017, doi: 10.1016/j.eswa.2016.10.052.

Mahmoud Dhimish (M'16) is Lecturer in Electronics and Control Engineering at the University of Huddersfield, UK. He graduated with M.Sc. in Electronics and Communication Engineering (Distinction) from the University of Huddersfield. Following this he gained a Ph.D. entitled "Fault Detection and Performance Analysis of Photovoltaic Installations" also from the University of Huddersfield. His current research interests include design, control, and performance analysis of photovoltaic systems.

Ghadeer Badran (M'19) is currently a research assistant at the University of Huddersfield, UK. She graduated with B.Sc. (Hons.) in Business Management from Princess Sumaya University of Technology, Jordan. She continued to work as research assistant on various projects related to renewable energy sector including techno-economic analysis of PV systems, and PV forecasting using artificial intelligence (AI) techniques. Her current research interests include data management, big data analysis, statistics and the AI-based systems.